Comparative analysis of the seismic behavior of low-rise buildings with hidden and drop beams

Carlos Zúñiga-Olvera[1], David Valverde-Burneo[1], Natividad García-Troncoso[1,2*], Christian E. Silva[1,3], Daniel Gómez P.[4], and Dan V. Bompa[5]

[1]Escuela Superior Politécnica del Litoral, ESPOL, Ecuador, caoczuni@espol.edu.ec, devalver@espol.edu.ec, nlgarcia@espol.edu.ec, chrsilva@espol.edu.ec

[2]Center of Nanotechnology Research and Development (CIDNA), Escuela Superior Politécnica del Litoral, ESPOL, Campus Gustavo Galindo Km 30.5 Vía Perimetral Guayaquil 090506

[3] Purdue University, School of Mechanical Engineering, West Lafayette, IN 47906, USA

[4] School of Civil Engineering and Geomatics, Universidad del Valle, Cali, Colombia

[5] School of Sustainability, Civil and Enviromental Engineering, University of Surrey, Guildford, UK

Abstract– This study presents a comparative analysis of two structural design concepts in the Ecuadorian construction market: hidden vs. drop beams. Typical structural systems used in low-rise buildings are special-moment frames, with either hidden or drop beams. The former is preferred by contractors and builders due to a notion of affordability, despite strong evidence of such system collapsing during recent earthquake events, particularly the April 2016 Ecuador earthquake (M7.8). This comparative analysis spans the mechanical, seismic, and economical aspects. A total of 32 structural models are developed and analyzed for linear and nonlinear static and dynamic response. Sixteen of these models are structures containing hidden beams, and the remaining 16 contain drop beams. The results show that structures with drop beams have no significant cost differences with hidden beams, while achieving a noticeable better structural behavior in high-risk seismic zones. The research gap that the present work aims to fill is a noticeable lack of previous studies comparing these two construction systems.

Keywords-- Hidden beam; Drop beam; Pushover analysis; Equivalent linearization; Moment-curvature relationship.

I. INTRODUCTION

Ecuador is considered a high seismic risk country [1]. Therefore, construction techniques and design procedures need to be performed carefully. Special moment frames are commonly utilized among the recommended structural systems according to the Ecuadorian Construction Code (NEC) [2]. However, there are two special moment-frame systems, described in NEC: 1) Special moment frame with drop beams, and 2) Special moment frame with hidden beams.

Despite being an important topic in Ecuadorian construction, there are limited studies comparing both structural systems. Few research studies are available in literature, mostly focused on feasibility analyses using special moment frames with hidden beams. Navyashree and Sahana [3] demonstrated that the hidden beam structures present up to three times more drift than drop beam buildings. This is largely expected in hidden beam floor systems because it has lower lateral stiffness than drop beam frames [4,5]. A comparative study conducted by [4]], where performance-based analysis of solid slabs on drop beams, ribbed slabs on shallow (hidden) beams, and flat

plates with or without drop panels, showed that models with drop beams offer enough mechanical properties to overcome lateral loads. An experimental study reported a comparison of flexural strength and deflection of hidden and drop beams [5]. Here, hidden beams surpassed the deflection limit, and they never achieved the same strength offered by a drop beam.

During the design process, hidden beams are designed to overcome higher seismic forces, compared to those affecting drop beams due to the "R" factor [2], [6]. Interstory drift, concrete strength, and the "R" factor are important parameters considered in some seismic vulnerability index methodologies of reinforced concrete buildings [7]–[9]. Typically, drop beam depth is limited by the architectural design. On the other hand, the depth of hidden beams is limited by the slab depth within the system. Thus, the only way to match the stiffness of a hidden beam system with a drop beam system is by increasing its width.

The proposed study uses the load resistance factor design method (LRFD). Hidden beams have more rebar than drop beams due to its lower depth. Therefore, its curvature ductility is low, and such a system is considered to be of lower ductility, and it should be carefully used in seismic zones [9].

As shown previously, there are limited studies on this topic. These are either different loading conditions, and specific seismic design requirements not representative for the Ecuadorian seismic hazard risk. Moreover, some studies indicate a limited difference in response between systems [10]. Considering the lack of comparative detailed studies on such frame systems under seismic loading and cost differences, there is a need of studies focused on the advantages and behavior of using both systems in high-risk seismic zones. Results of this study are compared with the literature review mentioned above.

II. METHODOLOGY

A 3D model of a 3-story building is used to compare hidden vs. drop beam systems, shown in Fig. 1. This model does not consider any plan or elevation irregularities, to not impact the global results by adding torsional forces. The seismic force is assumed only with 5% of accidental torsion to evaluate the translation behavior of each model. Some codes are considered to carry out this study. Ref. [2] is used to determine the seismic

demands, and to compare the interstory drift results with the maximum allowed values. References [11], [12] are used to design the concrete structural elements, such as beams and columns.
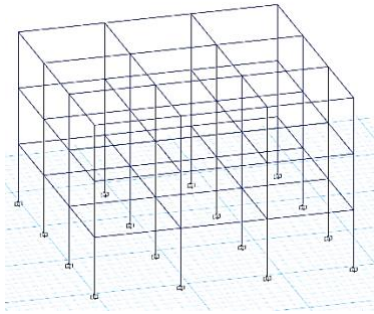

Fig. 1 3D model

Hidden beam and drop beam schematics are shown in Fig. 2. The distance between floors for this model is 3 m, resulting in an overall 9 m building. The plan configuration has a regular grid in both directions, with three spans of 4.5 m between axes. To compare both structural systems, the models are made with different cross-sections of the structural elements, both in beams and columns. The columns have squared cross-sections, and the beams have different sections depending on the beam type. In both hidden and drop beam type structures, the depth is upgraded in increments of 5 cm (see Tables I, and II).
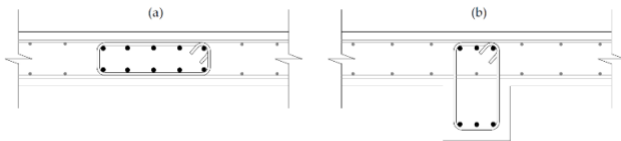

Fig. 2 a) Hidden beam section; b) Drop beam section.

TABLE I
LIST OF DROP BEAM MODELS

Beam Section	Column Section			
	C40x40	C45x45	C50x50	C55x55
B25x35	Model #1	Model #2	Model #3	Model #4
B25x40	Model #5	Model #6	Model #7	Model #8
B25x45	Model #9	Model #10	Model #11	Model #12
B25x50	Model #13	Model #14	Model #15	Model #16

TABLE II
LIST OF HIDDEN BEAM MODELS

Beam Section	Column Section			
	C40x40	C45x45	C50x50	C55x55
H35x25	Model #17	Model #18	Model #19	Model #20
H40x25	Model #21	Model #22	Model #23	Model #24
H45x25	Model #25	Model #26	Model #27	Model #28
H50x25	Model #29	Model #30	Model #31	Model #32

A. *Elastic analysis according to NEC*

The same procedure for analysis and structural design is conducted in the 32 models shown in Tables I and II. The results obtained are used to calculate interstory drifts, rebar requirements, and structure costs, according to references [11],

[12]. The seismic demand is then obtained from the elastic response spectrum of Guayaquil city, presented in Fig. 3, assuming a soil type: D, [2]. The base shear force is determined with an importance factor of 1, a mass source equal to 100% of the total dead load, and a spectral acceleration according to the fundamental period obtained from reference [2] which is 0.397 s. To compare both systems, all models are analyzed with the same seismic acceleration. The structural analysis and design are conducted considering seismic response modification factors of 8 and 5 for drop and hidden beams, respectively.
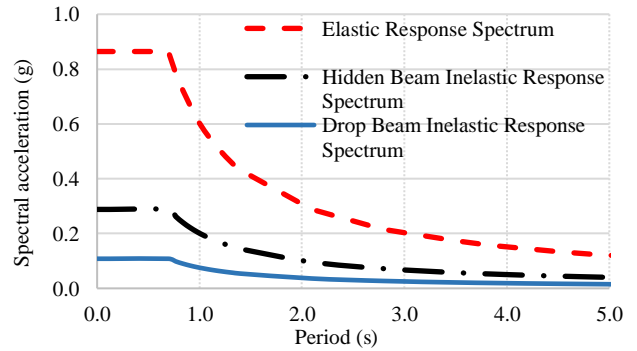

Fig. 3 Response spectrum according to Ecuadorian Code.

Materials assumed for this study are $f_c' = 21$ MPa concrete and $f_y = 420$ MPa rebar steel. A two-way ribbed slab is modeled as a "thin shell" type element of 0.25 m total depth, as presented in Fig. 4. The reason for this design decision is to transmit torsion to the beams and, thus, determine if the beams comply with the shear stress requirements due to shear force and torsion [12]. The moment of inertia is modified according to the structural element, 0.3 for hidden beams and two-way ribbed slabs, 0.5 for drop beams and 0.8 for columns according to NEC guidelines. Gravitational loads of 6 kN/m² and 2 kN/m² are defined for superimposed dead and live loads, respectively. The lateral seismic force is assigned to rigid diaphragms. All the restraints are assumed as perfect rigid restraints and the beam-column connections have a rigid-zone factor of 50% at the end-length offsets. Elements are designed according to the following load combinations.
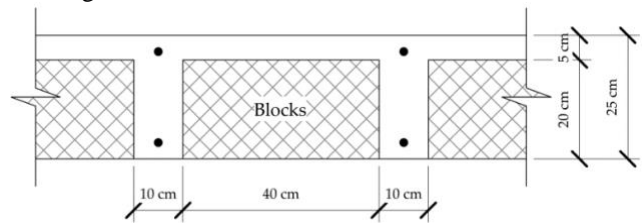

Fig. 4 Two-way ribbed slab cross-section.

$$1.4D \qquad (1)$$

$$1.2D + 1.6L \qquad (2)$$

$$1.2D + 1.0L + 1.0E \qquad (3)$$

$$0.9D + 1.0E \qquad (4)$$

B. Cost estimate

For the cost comparison, the take-off of materials such as concrete and reinforcement rebar is obtained from the design process. The cost index is used for comparison purposes to simplify the data obtained from the estimated budget. This metric takes values between 1 and 2, where 1 represents the lowest budget of all the analysed structures, and 2 is the highest. The slab structure is composed of 21 MPa concrete hollow blocks, for weight-lightening purposes, and top and bottom layers of one 12 mm, $f_y = 420$ MPa steel rebar per rib. Additionally, a slab cost reduction factor is considered due to the shoring procedure of hidden beams. The costs incurred in the concrete slab construction (labor included), both for hidden and drop beams is shown in Table III. The structural costs for beams and columns are estimated according to Ecuadorian unit costs [13].

TABLE III
MATERIAL COSTS FOR SLAB (CURRENCY: US DOLLAR)

Material	Qty.	Hidden Beam Slab Unit Cost	Drop Beam Slab Unit Cost	$/m2 for Hidden Beam Slab	$/m2 for Hidden Beam Slab
Concrete $f'_c = 21$ MPa	0.122 m³/m²	$ 215.0	$ 225.0		
Blocks	8 U/m²	$ 0.8	$ 0.8	$ 49.9	$ 51.1
Rebar Steel $f_y = 420$ MPa	9.04 kg/m²	$ 1.9	$ 1.9		

TABLE IV
MATERIAL COSTS FOR COLUMNS AND BEAMS (CURRENCY: US DOLLAR)

Material	Unit Cost	Unit
Rebar Steel $f_y = 420$ MPa	1910.0	$/Ton
Concrete $f'_c = 21$ MPa	254.0	$/m³

C. Non-linear analysis

With the information obtained from the design phase, plastic hinge behavior is defined to perform a non-linear pushover analysis. Plastic hinges are assigned, based on the ASCE 41-17 Standard [14], at both ends of the span of each structural element of the building models. This procedure is carried out to push the structure laterally with a load pattern related to the elastic lateral seismic force, corresponding to the model under analysis. The lateral load pattern obeys the following relationship: [2].

$$F_x = \frac{w_x h_x^k}{\sum_{i=1}^n w_i h_i^k} , \qquad (5)$$

where F_x is the applied lateral force in the x-th story, n the number of stories, w_x is the weight applied to the x-th story, w_i the weight applied to the i-th story, h_x is the height of the x

story, h_i the height of the i-th story, and k is the period coefficient, which is 1.

A series of pushover curves are obtained with the reinforcement rebar and sectio calculated on the design process. Moreover, the corresponding response elastic spectra are also computed using the FEMA 440 method. As a result, the performance points of models with H35x25, B25x35, H45x25, and B25x45 are calculated according to [15], [16]. In addition, base shear, roof displacement, vibration period, and effective damping are obtained to compare the global behavior of buildings with hidden and drop beam systems.

Next, a local analysis is carried out to compare the non-linear behavior of the hidden and the drop beam sections, using the reinforcement information of the most demanded beams of models 9, 12, 25 and 28. Then, the local behavior of hidden and drop beams is compared through moment curvature diagrams. First, stress-strain behavior of materials is defined for confined and unconfined concrete, whose curves are obtained according to reference [17]. Furthermore, the stress-strain diagram of reinforcement steel is defined in the model developed by [18]. Using static equilibrium and deformation compatibility conditions of materials, the nominal moment and curvature of the section are determined, thus obtaining the moment-curvature diagram [19], [20].

$$f'_c = \begin{cases} f'_c \left[\frac{2\varepsilon}{\varepsilon_{co}} - \left(\frac{\varepsilon}{\varepsilon_{co}} \right)^2 \right] & 0 \leq \varepsilon \leq \varepsilon_{co} \\ f'_c [1 - Z(\varepsilon - \varepsilon_{co})] & \varepsilon_{co} \leq \varepsilon \leq \varepsilon_{20c} \\ 0.2 f'_c & \varepsilon \geq \varepsilon_{20c} \end{cases} . \qquad (6)$$

All the variables and corresponding values appearing in Eq. (6) are defined in Table V. For the case of reinforcement steel stress-strain curve, it is defined in Eqns. (7), (8), (9).

$$f_s = \left[\frac{m(\varepsilon_s - \varepsilon_{sh}) + 2}{60(\varepsilon_s - \varepsilon_{sh}) + 2} + \frac{(60 - m)(\varepsilon_s - \varepsilon_{sh})}{2(30r + 1)^2} \right] , \qquad (7)$$

where m and r are:

$$m = \frac{(f_{su}/f_y)(30r + 1)^2 + 60r - 1}{15r^2} , \qquad (8)$$

$$r = \varepsilon_{su} - \varepsilon_{sh} , \qquad (9)$$

Similarly, the variables in Eq. (7) are defined in Table V.

TABLE V
CONCRETE AND REINFORCEMENT STEEL STRESS-STRAIN VARIABLES

	Description	Adopted values
f'_c	Compressive	21
ε_{co}	Unconfined concrete strain	0.002
ε_{cm}	Unconfined concrete maximum strain	0.004
f_y	Yield stress of longitudinal rebar (Mpa)	420
f_{su}	Maximum stress of longitudinal rebar (MPa)	630
E_S	Rebar Modulus of elasticity (MPa)	204080
ε_y	Strain of longitudinal rebar at yield	0.00206
ε_{sh}	Strain at start of hardening of rebar	0.01235
ε_{su}	Maximum strain of longitudinal rebar	0.07409
f_{yh}	Yield stress of stirrups (MPa)	420
ε_{shu}	Maximum strain of stirrups	0.07409
d_{bh}	Stirrup diameter (mm)	10

The ductility due to the curvature of the different sections is computed through:

$$U = \frac{\varphi_u}{\varphi_y} , \qquad (10)$$

where φ_u is the ultimate curvature, and φ_y is the yield curvature of the section. According to [20], the yield curvature considers the first yield of the tensile rebar, and for the ultimate curvature, this corresponds to the failure point, that is the last point in the moment-curvature diagram.

Since seismic-resistant design codes emphasize that beams should not fail due to shear actions there are some types of failure that control the flexural behaviour of beam sections, these are: failure due to crushing of the concrete by rupture of the stirrups (concrete loses the confinement and fails due to crushing), and tensile rupture of the longitudinal rebar. To consider the latter, the moment-curvature diagram must be interrupted when the unit strain of the tensile rebar exceeds ε_{su}. While considering the former, the moment-curvature diagram must be interrupted when the unit strain of the compression concrete exceeds ε_{cu}, [20], which is established by:

$$\varepsilon_{cu} = 0.004 + \frac{1.4 p_s f_{yh} \varepsilon_{sm}}{f'_{cc}} , \qquad (11)$$

where p_s is the volumetric ratio of confined steel, $p_s = p_x + p_y$. In this case, since we are using the Kent & Park model for confined concrete, thus $f'_{cc} = f'_c$. This Kent & Park model is commonly used on elements with high levels of confinement, such as columns. However, [21], [22] used this model to consider the confinement on beams caused by the transversal reinforcement. It is expected to have higher capacity and ductility on drop beams than on hidden beams [9].

III. RESULTS AND DISCUSSION

A. Interstory drift

As shown in Fig. 5 (drop beams), the maximum interstory drift value occurs in Model #1 with 1.66%, and the minimum value of 0.6% appears in Model #16. These results suggest that a depth increase in drop beams is equivalent to an increased column section, which is evident in isoline slopes. The maximum interstory drift in hidden beams appears in Model #17, with 3.25%, and the minimum of 1.81% occurs in Model #32. When comparing the slopes of both cases, drop beams show lower slopes which demonstrate the effectiveness of drop beams when compared with hidden beams
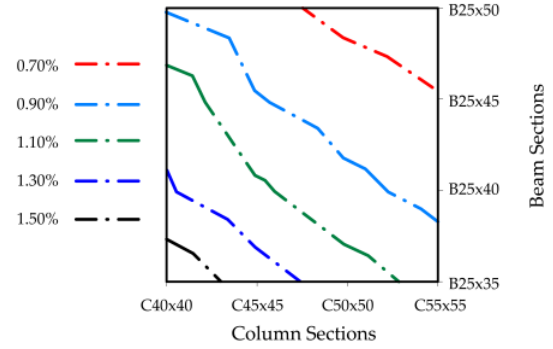

Fig. 5 Interstory drift results of drop beam models.

A closer look to the data presented in Figs. 5 and 6 indicates that a 0.05 m depth increase in drop beams is equivalent to a 0.15 m width increase in hidden beams. These results show that the influence of drop beams depth is threefold over hidden beam width [10]. It should be noted that the present study considers interstory drift limits as per the NEC: All drop beam models have a maximum interstory drift of less than 2%, which is the maximum allowed by the referred code. Regarding the hidden beam system, only three models comply with the Ecuadorian Code: Models #24, #28 and #32. Based on the obtained results from the elastic analysis, it is found that the maximum drifts obtained in drop beam models were two to three times lower than those obtained in hidden beam models.
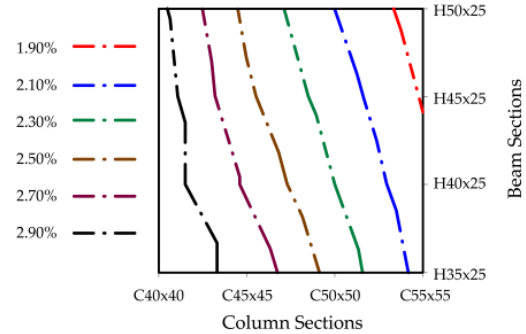

Fig. 6 Interstory drift results of hidden beam models.

For comparison purposes, another interstory drift analysis was completed with the addition of hidden beams without modified flexural rigidity. Here, Models #4, #8, #12, #16, #20, #24, #28 and #32 were considered. Interstory drifts of hidden beam models without considering modified flexural rigidity show values between 0.91% and 1.05% . Drop beams interstory drift values are between 0.60% and 1.04%. This comparison demonstrate that even without considering cracking in hidden beams, these will offer higher interstory drift values.

B. Cost comparison

According to the structural design, the columns have the reinforcement shown in Table VI which summarizes the longitudinal reinforcements of columns.

TABLE VI
LONGITUDINAL REINFORCEMENT FOR COLUMNS

Column Section	Rebar Provided	Total Rebar Area (cm2)	ρ (%)
40x40	8ø18mm	20.32	1.27%
45x45	8ø18mm	20.32	1.00%
50x50	12ø18mm	30.48	1.22%
55x55	12ø18mm	30.48	1.01%

Figure 7 shows the cost index for different structural sections. The results presented here show that the maximum cost index is 1.89 for a combination of a C55x55 column paired with a B25x50 beam, and the minimum cost index of 1 occurs for a combination of a C40x40 column with a B25x35 beam. Notice the change of column sections, where it is shown that the cost index increased around 30% between C45x45 and C50x50. This may be due to the change of the minimum longitudinal reinforcement on the columns (Table VI).
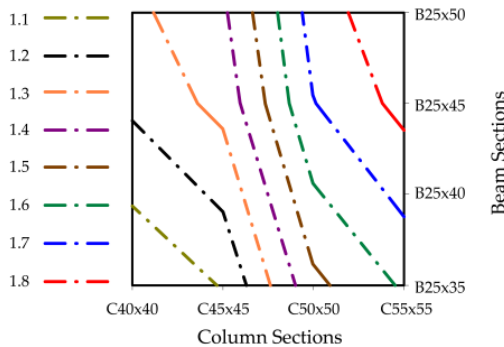

Fig. 7 Cost index of drop beam models.

A similar situation is observed in the hidden beam case, whose cost index chart is shown in Fig. 8. The most significant difference is the maximum cost index, which reaches a value of 2 for a combination of C55x55 column with an H50x25 beam. According to the interstory drift analysis, the models that comply with the Ecuadorian code are Model #24, Model #28, and Model #32. The cost differences with drop beam equivalent models are between 1% and 2% (Table VII), representing a negligible cost factor. A summary of superstructure difference and costs are shown in Tables VII and VIII respectively.
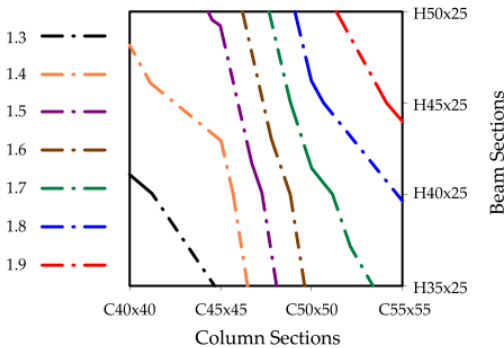

Fig. 8 Cost index of hidden beam models.

TABLE VII
COST DIFFERENCE BETWEEN DROP AND HIDDEN BEAM MODELS

Drop Beam Model	Hidden Beam Model	Cost Difference %
Model #1	Model #17	5.71%
Model #2	Model #18	5.01%
Model #3	Model #19	3.09%
Model #4	Model #20	2.32%
Model #5	Model #21	4.02%
Model #6	Model #22	2.85%
Model #7	Model #23	1.22%
Model #8	Model #24	1.07%
Model #9	Model #25	3.23%
Model #10	Model #26	1.89%
Model #11	Model #27	1.26%
Model #12	Model #28	1.43%
Model #13	Model #29	3.12%
Model #14	Model #30	2.73%
Model #15	Model #31	2.14%
Model #16	Model #32	1.83%

TABLE VIII
TOTAL COST FOR BUILDING STRUCTURE

Structural System	Beam Sections	Column Sections			
		C40x40	C45x45	C50x50	C55x55
Drop Beams	B25x35	$ 56,848	$ 58,797	$ 65,460	$ 68,023
	B25x40	$ 58,930	$ 60,887	$ 67,531	$ 70,079
	B25x45	$ 60,906	$ 62,852	$ 69,502	$ 71,993
	B25x50	$ 61,859	$ 63,766	$ 70,377	$ 73,026
Hidden Beams	H35x25	$ 60,092	$ 61,743	$ 67,483	$ 69,601
	H40x25	$ 61,301	$ 62,620	$ 68,352	$ 70,826
	H45x25	$ 62,872	$ 64,042	$ 70,380	$ 73,023
	H50x25	$ 63,787	$ 65,509	$ 71,882	$ 74,360

A comparison of interstory drifts and costs shows that Model #1 and Model #32 present similar interstory drifts. From a seismic design standpoint, these two models also have similar behaviour, with a difference of 9% between interstory drifts but with a 31% difference in costs. Since the results show that constructing buildings with drop beams instead of hidden beams is more economical and the interstory drift is small, the data implies that it is more cost-effective and technically feasible. At the same time, a lower interstory drift implies that the repair costs of the building after a seismic event are also lower.

C. Non-linear static analysis

The nonlinear static analysis is conducted using the ASCE 41-17 modelling parameters for beams and columns [14]. A FEMA 440 equivalent linearization is used to determine the performance points and global parameters from the nonlinear static analysis [15].

Next, the global ductility ratios are compared between hidden beam (red) and drop beam (blue) models. The results in Fig. 9 suggest that drop beam models have 50% higher ductility values than in those with hidden beams. This result is probably due to the greater depth and the lower amount of rebar required by the drop beams. Thus, drop beam structures have better seismic behaviour when compared to hidden beam models, [23]. Width changes of hidden beams do not affect the system

ductility. On the contrary, increasing the drop beam depth will significantly increase the system ductility ratio.
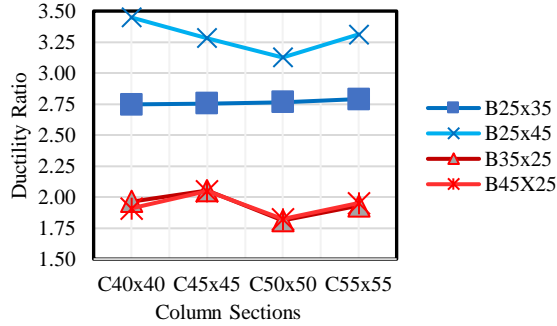

Fig. 9 Global ductility ratio.

The effective period is a parameter also considered in this study. Figure 10 show a comparison of the effective period for different beam/column combinations, where B refers to a drop beam and H to a hidden beam. Hidden beam models show a higher effective period than drop beam models. This result suggests that buildings with hidden beams will present lower lateral stiffness after the earthquake.
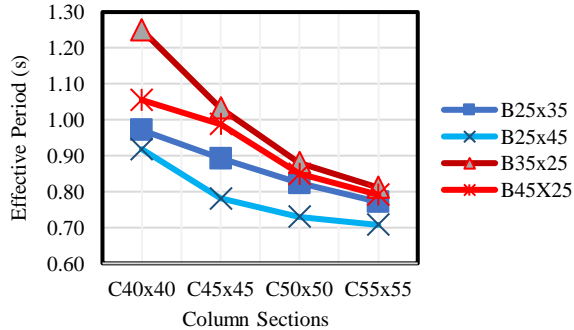
Fig. 10 Effective period results.

Figure 11 shows the differences in damping ratios for different beam/column combinations. The percentage of damping is higher in models containing drop beams (133%) than in buildings containing hidden beams (63%). This allows drop beam model buildings to better dissipate the effects of earthquakes in the nonlinear range.
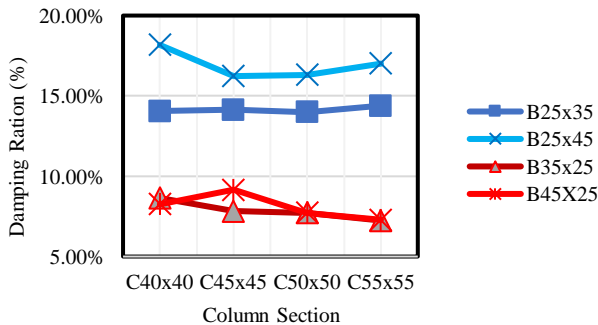

Fig. 11 Damping ratio results.

D. Capacity curves and performance points

Performance points obtained from the nonlinear static analysis following FEMA-440, exhibit differences in base shear and displacement values, according to the pushover curves of Figs. 11 and 12. Values of base shear for H35x25 hidden beam section are between 907.70 kN and 1272.70 kN, which can be compared with the B25x35 drop beam pushover curve that shows base shear values between 951.93 kN and 1667.62 kN. According to these results, drop beam systems offer higher base shear, with a mean difference of 5.5%. In terms of displacement, drop beam systems evidence lower displacements with a mean difference of 15.6%.
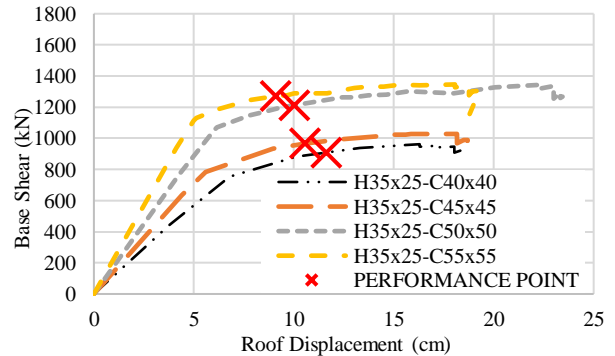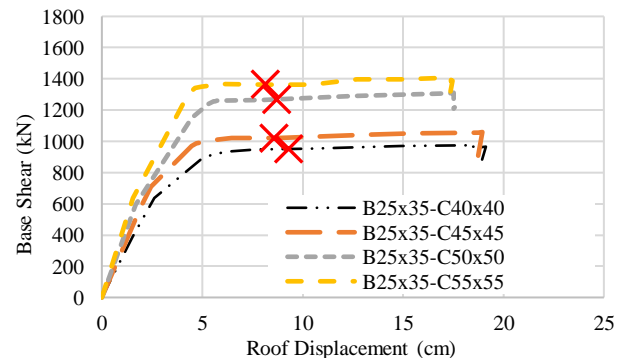

Fig. 12 H35x25 Pushover curves.

Fig. 13 B25x35 Pushover curves.

Comparing non-linear static results of H45x25 and B25x45 models, higher differences are observed in the pushover curves presented in Figs. 14 and 15. Here, the base shear of the H45x25 models is between 999.68 kN and 1394.60 kN, which is 23.8% lower than that of B25x45 drop beam model. Therefore, drop beam models show higher base shear values, and the differences increase as the beam depth increases. Regarding displacements, it can be observed that drop beam models have 20% lower displacements than hidden beam models. These results demonstrate a better seismic performance of drop beam systems instead of hidden beam systems.
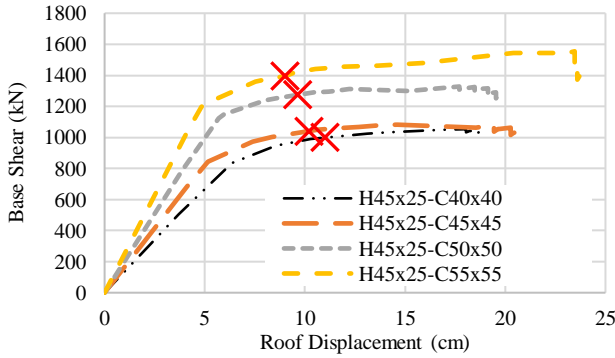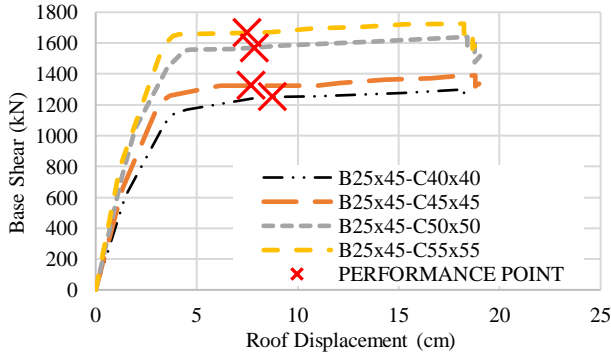
Fig. 14 H45x25 Pushover curves.

Fig. 15 B25x45 Pushover curves.

A summary of performance points is presented in Fig. 16 where Fx is the base shear obtained by the model and $Fmin$, is the minimum base shear obtained by the 16 analysis models, out from which eight are hidden beam models and the other eight are drop beam models. On the other axis, Ux and $Umin$ are the roof displacement and minimum roof displacement of the 16 models, respectively. The analysis shows that the effect of stiffness on beam and column sections represents a decrease in displacements and an increase in base shear values. The displacement ratio defined by $Ux/Umin$ shows that buildings with hidden beams deform about 55% more than buildings with drop beams with respect to the model with beam section B25x45 and columns of C55x55. At the same time, the stiffer buildings support higher basal shears with lower deformations, i.e., they have better seismic behaviour, confirming the results found in reference [10].
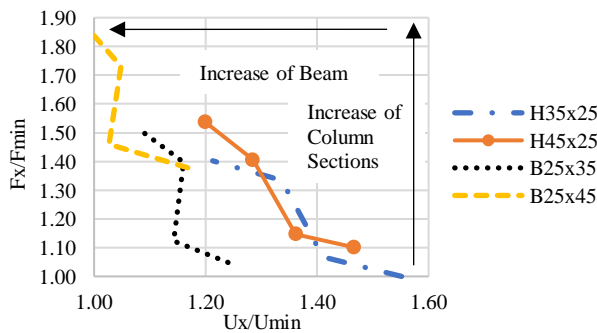

Fig. 16 Performance point curves.

E. Beam section comparison (material non-linearity)

To compare hidden and drop beam sections, several moment-curvature diagrams are generated from beams with the highest longitudinal reinforcement ratios and overlapped in Fig. 17. Main factors that affect moment-curvature diagrams are the beam cross-section, longitudinal reinforcement ratio, and stirrup spacing. Results suggest that drop beams have maximum moment values 20%-30% higher than hidden beam sections, similar results are reported in other study [24]. As expected, the section ductility in drop beams is also higher than in hidden beams due to their lower longitudinal reinforcement ratio. Drop beam section ductility is approximately 30% higher than hidden beam, which demonstrates its advantages in terms of stiffness, ductility, steel reinforcement, and flexural capacity (see Table IX) [9], [19], [20].
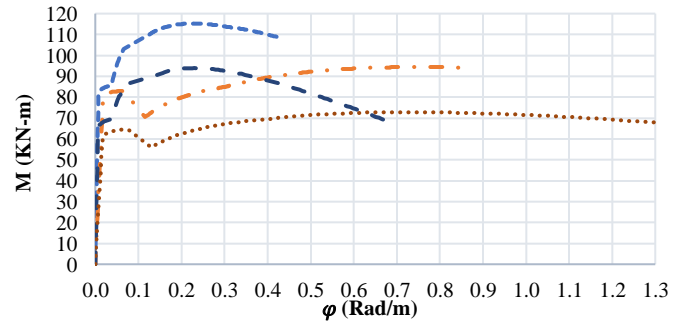
Fig. 17 Moment-Curvature diagrams.

TABLE IX
MOMENT-CURVATURE RESULTS

Structural System	Parameters	Column Section	
		C40X40	C55X55
	Model #	9	12
	φ_y (Rad/m)	0,0072	0,007
Drop beams B25x45	φ_u (Rad/m)	0,4332	0,6784
	Curvature Ductility U	60,17	96,91
	M_{max} (KN-m)	115,24	93,96
	Model #	25	28
	φ_y (Rad/m)	0,0181	0,0176
Hidden beams H45x25	φ_u (Rad/m)	0,8438	12,973
	Curvature Ductility U	46,62	73,71
	M_{max} (KN-m)	94,41	72,8

IV. CONCLUSIONS

A comparison of a low story building with two structural systems, hidden beams and drop beams was conducted using linear static, nonlinear static, moment curvature and structure budget analyses and the findings show that from models with

hidden beams, only three complied with the maximum allowable interstory drift established in the Ecuadorian Construction Code. The remaining 13 hidden beam models showed interstory drifts exceeding the maximum allowable 2%. The drift parameter could only be controlled using the stronger columns. In contrast, all the drop beam models complied rigorously with the allowable drift limit, ranging from 1.66% to 0.60%. This comparison suggests that the drop beam system withstands less damage than the hidden beam system during an earthquake event.

No significant differences between the cost associated to models with drop beams, versus those with hidden beams could be established. Although it is notorious that the models of buildings with hidden beams require a greater amount of rebar. However, this cost increment is compensated through the reduction on labor costs associated with the beams and slabs assemblies of the same formwork surface.

Comparing the models that comply with the maximum allowable interstory drift, the cost difference between both systems is noticeable. Hidden beam models #24, #28, and #32 comply with the standard. Furthermore, since any drop beam building models meet the maximum allowable interstory drift parameter, a price comparison can be made with any of these models, even Model #1. Thus, it could be estimated that the price of a hidden beam building is as much as 31% higher than the price of a drop beam building.

Global parameters show a better behavior on drop beams than on hidden beams. The damping ratio is lower in hidden beam models than in drop beam, which suggests that a drop beam system has more dissipation capacity than a hidden beam system. Ductility wise, the ratios obtained show higher ductility ratios in drop beam systems than hidden beam ones, which is also related with the R factor.

Pushover analysis results show that base shear values in drop beam models are higher than in hidden beam models, which demonstrates that the drop beam system is capable to withstand higher seismic lateral forces. Additionally, performance point displacements are lower in drop beam than in hidden beam models. Comparing the local behavior of hidden beams and drop beams, it is evident that drop beam systems can reach higher displacement values and higher flexural strengths than hidden beam systems, suggesting that the latter are safer than the former.

ACKNOWLEDGMENT

REFERENCES

[1] C. Beauval *et al.*, "A new seismic hazard model for Ecuador," *Bulletin of the Seismological Society of America*, vol. 108, no. 3A, pp. 1443–1464, 2018.

[2] NEC, "Peligro Sísmico. Diseño Sismo Resistente NEC-SE-DS." Quito: MIDUVI, 2014.

[3] K. Navyashree and T. S. Sahana, "Use of flat slabs in multi-storey commercial building situated in high seismic zone," *International Journal of Engineering Research & Technology*, vol. 3, no. 08, pp. 439–451, 2014.

[4] H. Samir, "Drop or Hidden Beams vs. Flat Slabs, which Way is Forward, A Performance Based Colloquial Narration," *International Journal of Engineering Research & Technology (IJERT)*, 2021.

[5] E. Özbek *et al.*, "Behavior and strength of hidden Rc beams embedded in slabs," *Journal of Building Engineering*, vol. 29, p. 101130, 2020.

[6] P. Rovello and V. Andrea, "Verificación del factor de reducción sísmico R, para el análisis inelástico de estructuras de hormigón armado de acuerdo al NEC-11.," 2014.

[7] M. M. Kassem, F. M. Nazri, E. N. Farsangi, and B. Ozturk, "Improved Vulnerability Index Methodology to Quantify Seismic Risk and Loss Assessment in Reinforced Concrete Buildings," *Journal of Earthquake Engineering*, vol. 26, no. 12, pp. 6172–6207, 2022, doi: 10.1080/13632469.2021.1911888.

[8] M. M. Kassem, F. Mohamed Nazri, E. N. Farsangi, and B. Ozturk, "Development of a uniform seismic vulnerability index framework for reinforced concrete building typology," *Journal of Building Engineering*, vol. 47, p. 103838, 2022, doi: https://doi.org/10.1016/j.jobe.2021.103838.

[9] R. Aguiar, *Análisis sísmico por desempeño*, vol. 342. Centro de Investigaciones Científicas. Escuela Politécnica del Ejército, 2003.

[10] H. Samir and M. Diab, "Slabs with Hidden Beams, Facts and Fallacies," *Asian Journal of Engineering and Technology*, vol. 2, no. 4, 2014.

[11] NEC-SE-HM, "NEC-SE-HM. Estructuras de Hormigón Armado," Quito, EC, Dec. 2014.

[12] ACI 318R-19, "ACI 318R-19. Building Code Requirements for Structural Concrete : An ACI Standard ; Commentary on Building Code Requirements for Structural Concrete," Farmington Hills, MI, Dec. 2019.

[13] D. A. Arciniega Larrea and E. R. Suárez Coba, "Análisis comparativo económico-estructural de edificios de 6, 12 y 18 pisos, aplicando el Código Ecuatoriano de la Construcción (CEC-2002) y la Norma Ecuatoriana de la Construcción (NEC-15).," Quito, 2016., 2016.

[14] ASCE, *Seismic Evaluation and Retrofit of Existing Buildings*, ASCE/SEI 41-17. American Society of Civil Engineers, 2017. doi: 10.1061/9780784414859.

[15] FEMA-440, "FEMA 440. Improvement of nonlinear static seismic analysis procedures," Redwood City, CA, Jun. 2005.

[16]   C. Velásquez Londoño, "Evaluación experimental de la longitud de rotación plástica en vigas de hormigón parcialmente pretensadas," Universitat Politècnica de Catalunya, 2017.

[17]   D. C. Kent and R. Park, "Flexural members with confined concrete," *Journal of the structural division*, vol. 97, no. 7, pp. 1969–1990, 1971.

[18]   R. Park and T. Paulay, *Reinforced concrete structures*. John Wiley & Sons, 1991.

[19]   C. Córdova, "Diseño de estructuras de hormigón armado," *Universidad de Santiago de Chile*, 2015.

[20]   T. Paulay and M. J. N. Priestley, *Seismic design of reinforced concrete and masonry buildings*, vol. 768. Wiley New York, 1992.

[21]   R. G. Delalibera, "Análise teórica e experimental de vigas de concreto armado com armadura de confinamento," *Dissertagao de Mestrado, Escola de Engenharia de Sao Carlos, Universidade de Sao Paulo*, 2002.

[22]   C. G. Nogueira and I. D. Rodrigues, "Ductility analysis of RC beams considering the concrete confinement effect produced by the shear reinforcement: a numerical approach," *Latin American Journal of Solids and Structures*, vol. 14, pp. 2342–2372, 2017.

[23]   M. A. R. Sanchez Aguilar, "Diseño sísmico basado en desempeño para una edificación esencial de concreto reforzado," Instituto Tecnológico y de Estudios Superiores de Monterrey, Monterrey, N.L., 2010.

[24]   M. I. Nadagouda and G. Ravi, "Analytical study on Flexural behaviour of RCC slabs with concealed beams using ANSYS," *International Research Journal of Engineering and Technology*, 2017, [Online]. Available: www.irjet.net